J Therm Anal Calorim (2010) 101:417–422
DOI 10.1007/s10973-010-0776-y

New cadmium and rare-earth metal molybdato–tungstates with scheelite-type structure

E. Tomaszewicz · G. Dąbrowska

CCTA10 Special Issue

Abstract A new group of cadmium and rare-earth metal molybdato–tungstates with the formula $Cd_{0.25}RE_{0.50}\square_{0.25}(MoO_4)_{0.25}(WO_4)_{0.75}$ (RE = Pr, Nd, Sm–Dy, □—vacancies in cation sublattice) were synthesized by a high-temperature solid-state reaction between RE_2MoO_6 and $CdWO_4$ mixed at the molar ratio of 1:3. Powder X-ray diffraction measurements showed that obtained phases adopt the scheelite-type structure. The phases melt congruently in the temperature range of 1382–1458 K.

Keywords Cadmium tungstate · Rare-earths molybdates · Scheelite-type structure · DTA–TG curves

Introduction

Inorganic compounds doped with rare-earth ions are known as promising materials for many applications [1–7]. Among many inorganic oxosalts, doped double molybdates and tungstates with the scheelite-type structure play important part in the production of luminescent materials. These inorganic compounds are extensively used in: luminescent devices, such as fluorescent lamps, cathode ray tubes, diode laser pumped solid-state lasers, amplifiers for fibreoptic communication, etc. Many of these compounds show very high luminescence quantum yield, excellent chemical and thermal durability in air.

E. Tomaszewicz (✉) · G. Dąbrowska
Department of Inorganic and Analytical Chemistry,
West Pomeranian University of Technology,
Al.Piastów 42, 71-065 Szczecin, Poland
e-mail: tomela@zut.edu.pl

Depending on the size of RE^{3+} ion or the solid-state synthesis conditions (temperature and time of annealing, cooling rate), rare-earth metal molybdates (RE_2MoO_6) have been known to crystallize in three polymorphic modifications, with monoclinic (α), cubic (β) and tetragonal (γ) symmetries [8–14]. Lanthanum molybdate (La_2MoO_6), obtained in standard solid-state conditions (gradually increasing the temperature to 1523 K, keeping for 40 h at 1523 K and furnace cooling) adopts the tetragonal γ-form [10, 13]. Ce_2MoO_6 has a pseudo-cubic, fluorite-related structure (β-form), the parameters of which are still unknown [10, 13, 14]. The most characteristic type of structure for RE_2MoO_6 (RE = Y, Pr–Lu) is the one closely related to the scheelite-type (α-polymorph, *C2/c*; Z = 8) [8–13]. It consists of three, nonequivalent deformed cubes REO_8 joined by common edges. Connected to each other, deformed trigonal bipyramids MoO_5 form zigzag rows running along the [001] direction [12, 13].

This paper presents the synthesis of new cadmium and rare-earths molybdato–tungstates of the formula $Cd_{0.25}RE_{0.50}\square_{0.25}(MoO_4)_{0.25}(WO_4)_{0.75}$ (RE = Pr, Nd, Sm–Dy, □—vacancies in cation sublattice) from RE_2MoO_6 (α-forms) and $CdWO_4$. The obtained compounds were defined by XRD, SEM, TA and IR methods.

Experimental

Synthesis

The starting materials were RE_2MoO_6 (RE = Pr, Nd, Sm–Dy) and $CdWO_4$. Polycrystalline rare-earth molybdates were prepared by a solid-state reaction, used by other authors [15, 16], from stoichiometric amounts of analytical grade RE_2O_3 (RE = Nd, Sm–Gd, Dy), Pr_6O_{11}, Tb_7O_{12} and

MoO_3. The reagents were ground and annealed in conditions described previously [17]. In order to obtain $CdWO_4$, a stoichiometric mixture of CdO (99.9%, Fluka) with WO_3 (99.9%, Fluka) was thoroughly ground in an agate mortar and heated in static air, in 12-h cycles and at the temperatures: 1173; 1223; 1273; 1323; and 1373 K. To investigate the reactivity of RE_2MoO_6 with $CdWO_4$, the $CdWO_4$/RE_2MoO_6 mixtures were prepared with the range of cadmium tungstate from 10.00 to 90.00 mol%. All mixtures were heated in air, in ceramic crucibles and in a resistance furnace (temperature accuracy ± 1 K). The following thermal treatment conditions have been used: 1298 K (12 h); 1273 K (12 h); 1025 K (12 h); 1323 K (2 × 12 h) and 1343 K (2 × 12 h). For better reactivity, after each 12-h period of annealing, the mixtures were cooled to room temperature and ground in an agate mortar. Mass changes of all samples were checked.

Elucidation of experimental methods

X-ray powder diffraction patterns, performed to control the progress of a solid-state reaction, were collected within the range from 10° to 45° 2Θ with the step 0.02° and counting time 1 s/step on a HZG-4 diffractometer with Cu $K\alpha_{aver}$ radiation ($\lambda = 0.15418$ nm). For indexing, XRD patterns were collected within the range from 10° to 100° 2Θ with the step 0.02° and counting time 10 s/step. The POWDER program [18, 19] was used to obtain accurate unit cell dimensions.

The DTA–TG curves were obtained using a SDT 2960 TA Instruments thermoanalyzer. The experiments were carried out in air at the flow rate of 110 mL/min and at the heating rate of 10 K/min. The mass of each analyzed sample was about 40 mg.

The morphology of selected samples was determined using a JEOL JSM-1600 scanning electron microscope. The pressed samples were coated with thin gold–palladium alloy layer to facilitate conductivity.

IR spectra were recorded on a Specord M-80 spectrometer. The samples were pressed in pellets with KBr in the weight ratio of 1:300.

Results and discussion

Phase identification in the $CdWO_4$–RE_2MoO_6 (RE = Pr, Nd, Sm–Dy) system

The XRD patterns of the samples obtained after each heating period of all $CdWO_4$/RE_2MoO_6 mixtures were recorded and analyzed. Figure 1 presents XRD pattern of the initial mixture comprising 75.00 mol% of $CdWO_4$ and 25.00 mol% of Eu_2MoO_6 as well as the diffraction pattern of the sample obtained after the last heating cycle of this mixture. The XRD

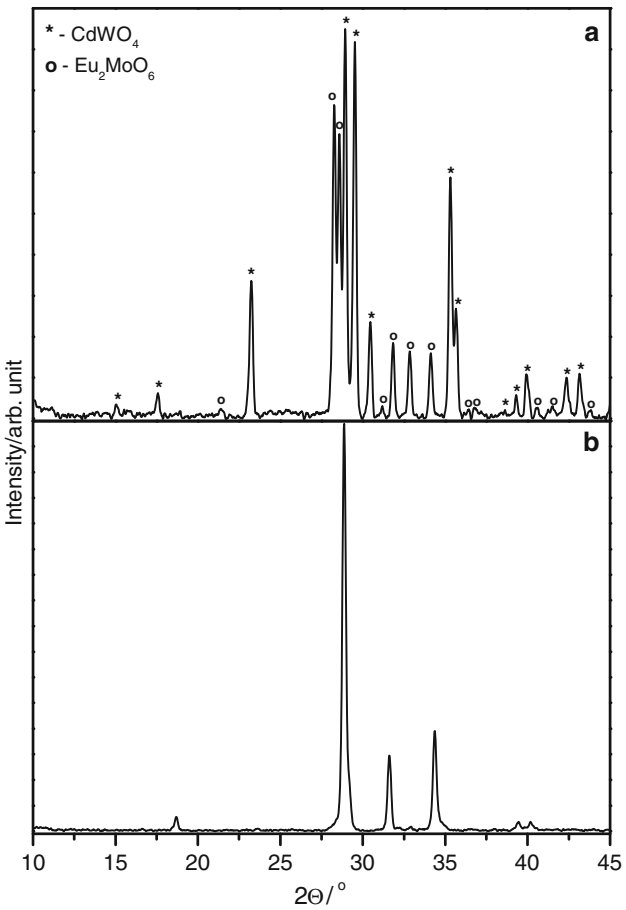

Fig. 1 XRD patterns of an initial $CdWO_4$/Eu_2MoO_6 mixture (the molar ratio of reagents 3:1) (**a**), the sample obtained after last heating cycle of this mixture (**b**)

results indicate that initial compounds react with each other in the solid state. The prepared samples, which initial mixtures contained 75.00 mol% of $CdWO_4$ and 25.00 mol% of RE_2MoO_6, were pure single phase and their XRD patterns showed only the diffraction lines characteristic of the scheelite-type structure. The diffraction patterns of the samples obtained after the last heating cycle and comprising initially below 75.00 mol% of $CdWO_4$ contained two sets of diffractions lines, i.e., the set of reflexions that can be attributed to an adequate RE_2MoO_6 and the set of diffraction lines characteristic for compounds with the scheelite-type structure. The same set of reflections as well as the set of diffraction lines characteristic for $CdWO_4$ were observed on the diffraction patterns of the samples obtained after heating $CdWO_4$/RE_2MoO_6 mixtures containing initially above 75.00 mol% of $CdWO_4$. We observed the mass decreases in all $CdWO_4$/RE_2MoO_6 mixtures after each heating period. The biggest values of total mass loss (calculated by adding the mass losses recorded after each heating period) were recorded for the samples comprising initially 75.00 mol% of $CdWO_4$ and 25.00 mol% of RE_2MoO_6 and they equaled: (*Pr*):

16.840%; (*Nd*): 16.680%; (*Sm*): 16.750%; (*Eu*): 16.640%; (*Gd*): 16.550%; (*Tb*): 16.540% and (*Dy*): 16.460%. The values of mass losses calculated on a base of the Eq. 1, equal: (*Pr*): 16.521%; (*Nd*): 16.450%; (*Sm*): 16.322%; (*Eu*): 16.289%; (*Gd*): 16.181%; (*Tb*): 16.147% and (*Dy*): 16.074%. Real values of mass losses are slightly higher than the calculated ones. This is because mass losses in experiment include also these (so-called "heat losses") observed at high temperatures.

$$3CdWO_{4(s)} + RE_2MoO_{6(s)} = 4Cd_{0.25}RE_{0.50}\square_{0.25}(MoO_4)_{0.25}(WO_4)_{0.75(s)} + 2CdO_{(g)} \quad (1)$$

The authors suggest that charge compensation, in the structures of obtained phases, takes place through a creation of statistical distributed vacancies in cation sublattice (marked as □).

Characterization of $Cd_{0.25}RE_{0.50}\square_{0.25}(MoO_4)_{0.25}(WO_4)_{0.75}$ by XRD, SEM, and IR methods

The results of indexing powder diffraction patterns of $Cd_{0.25}RE_{0.50}\square_{0.25}(MoO_4)_{0.25}(WO_4)_{0.75}$ as well as the values of interplanar distances for $CaWO_4$ [20] are shown in Table 1. The calculated lattice parameters, the values of experimental (obtained by degassing of samples and hydrostatic weighing in CCl_4 as pycnometric liquid) and calculated density for obtained compounds as well as for $CaWO_4$ and $CdMoO_4$ (both the scheelite-type structure) [20, 21] are shown in Table 2. The data collected in Tables 1 and 2 confirm that $Cd_{0.25}RE_{0.50}\square_{0.25}(MoO_4)_{0.25}(WO_4)_{0.75}$ are isostructural and crystallize in the tetragonal system, in the scheelite-type structure. The unit cell parameters of new cadmium and rare-earth metal molybdato–tungstates linearly decrease with increasing of atomic number of a lanthanide (Fig. 2).

Figure 3 shows the SEM morphology of $Cd_{0.25}Pr_{0.50}\square_{0.25}(MoO_4)_{0.25}(WO_4)_{0.75}$ particles. The edges of the grains are clear and the particles are in the shape of oval plates. Grains have different sizes, and the average particle size is about 8 μm.

IR spectra of $Cd_{0.25}RE_{0.50}\square_{0.25}(MoO_4)_{0.25}(WO_4)_{0.75}$ are shown in Fig. 4. In it the spectra of obtained compounds are very similar. In the literature on IR spectroscopy of solid single and double molybdates and tungstates with the

Table 1 Results of indexing $Cd_{0.25}RE_{0.50}\square_{0.25}(MoO_4)_{0.25}(WO_4)_{0.75}$ powder diffraction patterns

No.	*Pr*		*Nd*		*Sm*		*Eu*		*Gd*		*Tb*		*Dy*		*CaWO₄*		*h*	*k*	*l*
	d_{obs}/nm	I/I_0	d_{obs}/nm	I/I_0	d_{obs}/nm	I/I_0	d_{obs}/nm	I/I_0	d_{obs}/nm	I/I_0	d_{obs}/nm	I/I_0	d_{obs}/nm	I/I_0	d_{obs}/nm	I/I_0			
1	0.47703	5	0.47551	5	0.47475	5	0.47375	4	0.47275	6	0.47126	4	0.47002	4	0.47645	84	1	0	1
2	0.31125	100	0.31030	100	0.30956	100	0.30883	100	0.30841	100	0.30727	100	0.30655	100	0.31049	100	1	1	2
3	0.28676	21	0.28462	15	0.28374	22	0.28261	16	0.28208	20	0.28131	18	0.28045	21	0.28426	39	0	0	4
4	0.26218	34	0.26166	23	0.26114	30	0.26070	27	0.26040	25	0.25938	17	0.25880	22	0.26213	19	2	0	0
5	0.22964	4	0.22925	3	0.22880	2	0.22836	3	0.22808	4	0.22714	2	0.22670	3	0.22962	18	2	1	1
6	0.22676	3	0.22561	1	0.22497	3	0.22427	2	0.22395	3	0.22315	2	0.22257	3	0.22562	3	1	1	4
7	0.19993	2	0.19927	1	0.19873	2	0.19828	1	0.19791	1	0.19722	1	0.19681	1	0.19943	10	2	1	3
8	0.19349	38	0.19263	30	0.19210	42	0.19160	35	0.19134	38	0.19066	34	0.19017	33	0.19276	36	2	0	4
9	0.18536	11	0.18501	14	0.18466	16	0.18431	15	0.18407	16	0.18337	12	0.18299	13	0.18536	15	2	2	0
10	0.16992	25	0.16882	16	0.16831	19	0.16777	19	0.16746	18	0.16695	16	0.16648	21	0.16877	17	1	1	6
11	0.15924	21	0.15891	22	0.15859	29	0.15826	22	0.15809	30	0.15748	19	0.15713	24	0.15921	23	3	1	2
12	0.15567	12	0.15512	10	0.15474	13	0.15439	11	0.15418	11	0.15362	11	0.15325	10	0.15528	13	2	2	4
13	0.14332	3	0.14231	3	0.14179	3	0.14130	3	0.14105	3	0.14064	3	0.14021	3	0.14218	4	0	0	8
14	0.13100	4	0.13082	4	0.13057	4	0.13034	4	0.13019	4	0.12968	3	0.12942	3	0.13109	2	4	0	0
15	0.12567	8													0.12497	7	2	0	8
16	0.12523	10	0.12471	14	0.12440	16	0.12407	14	0.12389	17	0.12346	10	0.12315	14	0.12480	11	3	1	6
17	0.12064	5	0.12037	5	0.12018	7	0.11992	5	0.11984	4	0.11930	4	0.11901	4	0.12055	2	4	1	3
18	0.11918	4	0.11888	4	0.11862	5	0.11835	3	0.11822	6	0.11777	3	0.11751	4	0.1903	7	4	0	4
19	0.11720	5	0.11701	5	0.11679	5	0.11657	3	0.11645	6	0.11600	3	0.11574	4	0.11723	4	4	2	0
20	0.11340	4	0.11279	4	0.11247	4	0.11212	2	0.11196	4	0.11160	2	0.11130	3	0.11282	3	2	2	8
21	0.10956	4	0.10880	4	0.10845	4	0.10807	5	0.10788	4			0.10724	5	0.10873	3	1	1	10
22	0.10848	4	0.10822	7	0.10799	6	0.10777	6	0.10764	8	0.10723	5	0.10699	7	0.10837	5	4	2	4
23	0.10380	4	0.10341	4	0.10317	4	0.10292	3	0.10279	3	0.10242	2	0.10217	2	0.10352	2	3	3	6
24	0.10118	5	0.10100	5	0.10080	6									0.10118	3	5	1	2

Table 2 Crystallographic characteristic of $Cd_{0.25}RE_{0.50}\square_{0.25}(MoO_4)_{0.25}(WO_4)_{0.75}$, $CaWO_4$ and $CdMoO_4$

Compound	a/nm	c/nm	c/a	Z	V/nm^3	d_{exp}/g cm^{-3}	d_{cal}/g cm^{-3}	References
$Cd_{0.25}Pr_{0.50}\square_{0.25}(MoO_4)_{0.25}(WO_4)_{0.75}$	0.52415(1)	1.1468(6)	2.1880	4	0.31508(2)	6.50	6.92	This study
$Cd_{0.25}Nd_{0.50}\square_{0.25}(MoO_4)_{0.25}(WO_4)_{0.75}$	0.52332(2)	1.1383(9)	2.1753	4	0.31176(7)	6.64	7.02	This study
$Cd_{0.25}Sm_{0.50}\square_{0.25}(MoO_4)_{0.25}(WO_4)_{0.75}$	0.52236(5)	1.1344(2)	2.1717	4	0.30954(4)	6.72	7.12	This study
$Cd_{0.25}Eu_{0.50}\square_{0.25}(MoO_4)_{0.25}(WO_4)_{0.75}$	0.52137(1)	1.1303(2)	2.1680	4	0.30725(2)	6.79	7.18	This study
$Cd_{0.25}Gd_{0.50}\square_{0.25}(MoO_4)_{0.25}(WO_4)_{0.75}$	0.52067(1)	1.1283(7)	2.1671	4	0.30589(9)	6.86	7.25	This study
$Cd_{0.25}Tb_{0.50}\square_{0.25}(MoO_4)_{0.25}(WO_4)_{0.75}$	0.51873(5)	1.1250(5)	2.1688	4	0.30273(6)	6.93	7.34	This study
$Cd_{0.25}Dy_{0.50}\square_{0.25}(MoO_4)_{0.25}(WO_4)_{0.75}$	0.51762(1)	1.1216(4)	2.1669	4	0.30052(1)	7.03	7.42	This study
$CaWO_4$	0.524294(6)	1.1373(7)	2.1692	4	0.31264(6)	6.100	6.117	[20]
$CdMoO_4$	0.5156(1)	1.1196(1)	2.1715	4	0.2976(5)		6.078	[21]

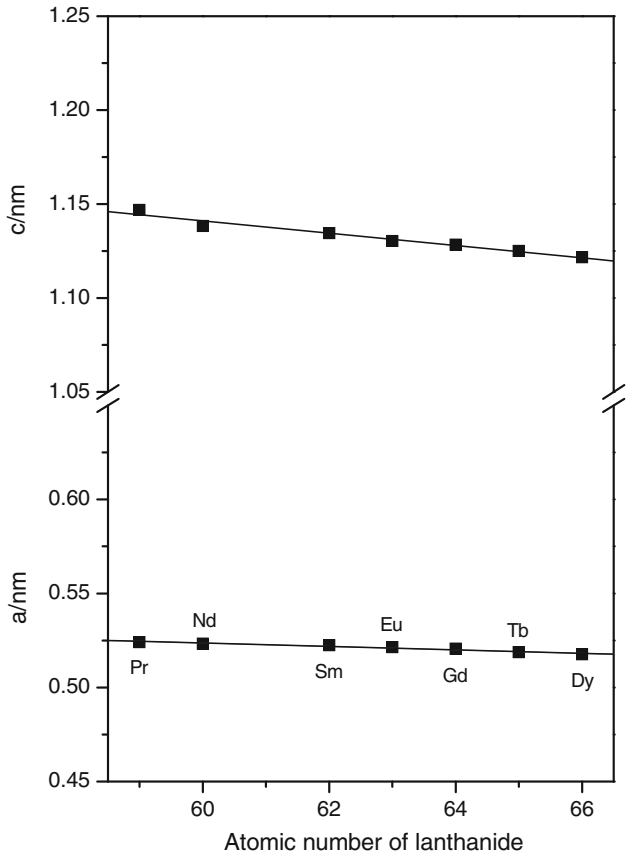

Fig. 2 Variation of lattice parameters for the $Cd_{0.25}RE_{0.50}\square_{0.25}(MoO_4)_{0.25}(WO_4)_{0.75}$ compounds with an atomic number of lanthanide

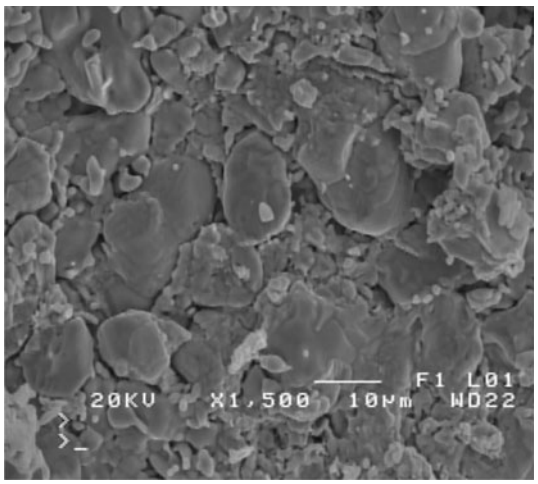

Fig. 3 SEM image of the $Cd_{0.25}Pr_{0.50}\square_{0.25}(MoO_4)_{0.25}(WO_4)_{0.75}$ sample

scheelite-type structure [22–26], the broad absorption bands with their maxima at ~928 cm^{-1} can be attributed to the symmetric modes of W–O bonds in WO_4 more than Mo–O bonds in MoO_4 (the region of vibration frequencies for WO_4—935–925 cm^{-1} while for MoO_4—905–894 cm^{-1} [22]). The broad absorption bands centred around 816 and 756 cm^{-1} the outcome of stretching vibrations of W–O bonds in WO_4 tetrahedra [22–26]. The absorption bands with the maxima located at ~440 and ~312 cm^{-1} can be ascribed as the symmetric and asymmetric deformation modes of W–O bonds in WO_4 tetrahedra, respectively [22–26]. Because of the small amount of MoO_4 against WO_4 tetrahedra in the structures of $Cd_{0.25}RE_{0.50}\square_{0.25}(MoO_4)_{0.25}(WO_4)_{0.75}$, the absorption bands connected with stretching as well deformation modes of Mo–O bonds in MoO_4 tetrahedra were not observed.

Thermal studies of $Cd_{0.25}RE_{0.50}\square_{0.25}(MoO_4)_{0.25}(WO_4)_{0.75}$

In order to specify thermal properties of $Cd_{0.25}RE_{0.50}\square_{0.25}(MoO_4)_{0.25}(WO_4)_{0.75}$, DTA–TG investigations were performed in air. Figure 5 shows DTA curves of these compounds. On each DTA curve only one endothermic effect was found. No mass losses were noted on the TG curves (not presented here) up to the onsets of the observed effects. On the base of DTA–TG curves for

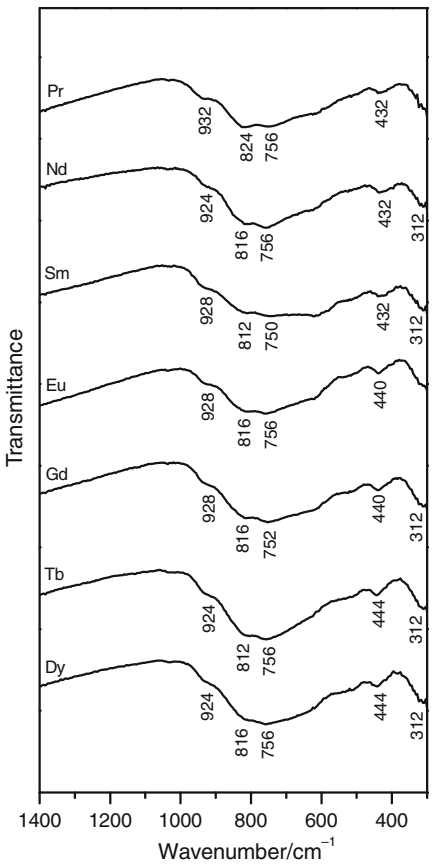

Fig. 4 IR spectra of $Cd_{0.25}RE_{0.50}\square_{0.25}(MoO_4)_{0.25}(WO_4)_{0.75}$

$Cd_{0.25}RE_{0.50}\square_{0.25}(MoO_4)_{0.25}(WO_4)_{0.75}$ and observations of the residues in corundum crucibles it was found that endothermic effects with their onsets at: 1382 K(*Pr*), 1420 K(*Nd*), 1450 K(*Sm*), 1458 K(*Eu*), 1454 K(*Gd*), 1448 K(*Tb*), and 1461 K(*Dy*) are associated with melting of these compounds. In order to determine melting behaviour of $Cd_{0.25}RE_{0.50}\square_{0.25}(MoO_4)_{0.25}(WO_4)_{0.75}$, additional tests were carried out. Samples of obtained compounds were heated in a furnace at the temperature higher about 10 K than the onsets of the recorded effects. After heating for 4 h, the samples were quickly removed from a furnace and rapidly quenched to 263 K. The XRD patterns of melted samples show only diffraction lines characteristic for initial phases. Therefore, the endothermic effects recorded on DTA curves of all obtained compounds are associated with congruent melting $Cd_{0.25}RE_{0.50}\square_{0.25}(MoO_4)_{0.25}(WO_4)_{0.75}$.

Conclusions

New cadmium and rare-earths molybdato–tungstates with the formula of $Cd_{0.25}RE_{0.50}\square_{0.25}(MoO_4)_{0.25}(WO_4)_{0.75}$ (RE = Pr, Nd, Sm–Dy, □—vacancies in cation sublattice) were prepared by a conventional solid-state sintering reaction from RE_2MoO_6 and $CdWO_4$. The obtained compounds are isostructural and crystallize in the tetragonal system, in the scheelite-type structure. The lattice parameters of the obtained compounds linearly decrease with

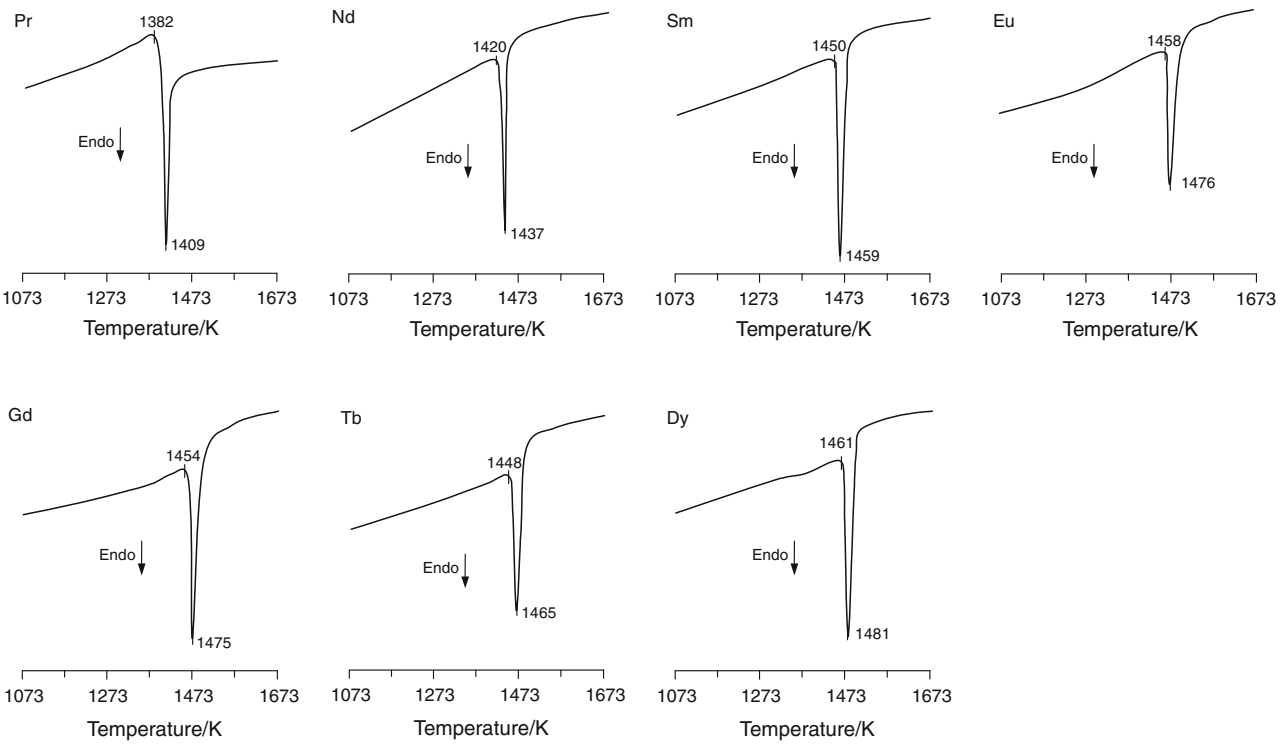

Fig. 5 DTA curves of $Cd_{0.25}RE_{0.50}\square_{0.25}(MoO_4)_{0.25}(WO_4)_{0.75}$

increasing of an atomic number of lanthanide. Big differences between the calculated and experimental values of density for each phases obtained confirm a presence of statistical distributed vacancies in cation sublattice. In air $Cd_{0.25}RE_{0.50}\square_{0.25}(MoO_4)_{0.25}(WO_4)_{0.75}$ melt congruently in the temperature range of 1382–1458 K. Due to congruent melting, the $Cd_{0.25}RE_{0.50}\square_{0.25}(MoO_4)_{0.25}(WO_4)_{0.75}$ crystals can be grown by Czochralski method. This fact makes the studied compounds promising materials for lasers.

Acknowledgements This scientific work is financed from the Polish Budget Resources allocated to science in the years 2009–2012 as the research project No. N N209 336937.

References

1. Wang Z, Liang H, Gong M, Su Q. Novel red phosphor of Bi^{3+}, Sm^{3+} co-activated $NaEu(MoO_4)_2$. Opt Mater. 2007;29:896–900.
2. Voron'ko YK, Subbotin KA, Shukshin VE, Lis DA, Ushakov SN, Popov AV, Zharikov EV. Growth and spectroscopic investigations of Yb^{3+}-doped $NaGd(MoO_4)_2$ and $NaLa(MoO_4)_2$—new promising laser crystals. Opt Mater. 2006;29:246–52.
3. Wang Z, Li X, Wang G, Song M, Wei Q, Wang G, Long X. Growth and optical properties of Ho^{3+}:$NaGd(MoO_4)_2$ crystal. Opt Mater. 2008;30:1873–7.
4. Wei Y, Tu Ch, Wang H, Yang F, Jia G, You Z, Lu X, Li J, Zhu Z, Wang Y. Optical properties of Nd^{3+}:$NaLa(WO_4)_2$ single crystal. Opt Mater. 2007;29:1653–7.
5. Demirkhanyan GG, Babajanyan VG, Kokanyan EP, Kostanyan RB, Gruber JB, Sardar DK. Spectroscopic properties of the $NaBi(WO_4)_2$:Yb^{3+} crystal. Opt Mater. 2007;29:1107–10.
6. Šulcová P, Vitásková L, Trojan M. Thermal analysis of the $Ce_{1-x}Tb_xO_2$ pigments. J Therm Anal Calorim. doi:10.1007/s10973-009-0129-x.
7. Pasierb P, Drożdż-Cieśla E, Gajerski R, Łabuś S, Komornicki S, Rękas M. Chemical stability of $Ba(Ce_{1-x}Ti_x)_{1-y}Y_yO_3$ proton-conducting solid electrolytes. J Therm Anal Calorim. 2009;96:475–80.
8. Blasse G. Dilanthanide molybdates and tungstates Ln_2MO_6. J Inorg Nucl Chem. 1966;28:1488–9.
9. Klevtsov PV, Kharchenko LY, Klevtsova RF. Crystallization and polymorphism of rare-earth oxymolybdates Ln_2MoO_6. Kristallografiya. 1975;20:571–578 (in Russian).
10. Brixner LH, Sleight AW, Licis MS. Ln2MoO6-type rare earth molybdates—preparation and lattice parameters. J Solid State Chem. 1972;5:186–90.
11. Tulin AV, Efremov VA. Polymorphism oxotungstates TR_2WO_6. Analysis of structure II-type (Gd_2WO_6 and Gd_2MoO_6). Mechanism of polymorphic transformation of Gd_2WO_6 (II ⇔ V). Kristallografiya. 1987;32:371–7. (in Russian).
12. Alonso JA, Rivillas F, Martinez-Lope MJ, Pomjakushin V. Preparation and structural study from neutron diffraction data of R_2MoO_6 (R = Dy, Ho, Er, Tm, Yb, Y). J Solid State Chem. 2004;177:2470–6.
13. Xue JS, Antonio MR, Soderholm L. Polymorphs of Ln_2MoO_6: a neutron diffraction investigation of the crystal structure of La_2MoO_6 and Tb_2MoO_6. Chem Mater. 1995;7:333–40.
14. Antonio MR, Staub U, Xue JS, Soderholm L. Comparison of the cation valence and coordination in Ce_2UO_6 and Ce_2MoO_6. Chem Mater. 1996;8:2673–80.
15. Belina P, Myšková V, Šulcová P. Comparison of the crystallisation and solid state reaction methods for the preparation of rare-earth orthophosphates. J Therm Anal Calorim. 2009;96:949–54.
16. Tomaszewicz E, Typek J, Kaczmarek SM. Synthesis, characterization and thermal behaviour of new copper and rare-earth metal tungstates. J Therm Anal Calorim. 2009;98:409–21.
17. Tomaszewicz E, Dąbrowska G. Reactivity in the solid state between $ZnWO_4$ and some rare-earth metal molybdates RE_2MoO_6 (RE = Y, Sm, Eu, Gd, Dy, Ho, Er and Lu). J Therm Anal Calorim. 2008;94:189–94.
18. Taupin D. General method of indexing powder patterns. J Appl Crystallogr. 1968;1:178–81. (in French).
19. Taupin D. A powder-diagram automatic-indexing routine. J Appl Crystallogr. 1973;6:380–5.
20. Blanchard FN. X-ray powder data for $CaWO_4$, synthetic scheelite. Powder Diff. 1989;4:220–2.
21. Daturi M, Busca G, Borel MM, Leclaire A, Piaggio P. Vibrational and XRD study of the system $CdWO_4$–$CdMoO_4$. J Phys Chem B. 1997;101:4358–69.
22. Tsaryuk VI, Zolin VF. Vibration and vibronic spectra of lanthanide compounds with different types of coordination polyhedra of tungsten and molybdenum. Spectrochim Acta A. 2001;57:355–9.
23. Hanuza J, Benzar A, Haznar A, Mączka M, Pietraszko A, Van der Maas JH. Structure and vibrational dynamics of tetragonal $NaBi(WO_4)_2$ scheelite crystal. Vib Spectr. 1996;12:25–36.
24. Hanuza J, Mączka M, Van der Maas JH. Polarized IR and Raman spectra of tetragonal $NaBi(WO_4)_2$, $NaBi(MoO_4)_2$ and $LiBi(MoO_4)_2$ single crystals with scheelite structure. J Mol Struct. 1995;348:349–52.
25. Clark GM, Doyle WP. Infra-red spectra of anhydrous molybdates and tungstates. Spectrochim Acta. 1966;22:1441–7.
26. Khanna RK, Lippincott ER. Infrared spectra of some scheelite structures. Spectrochim Acta A. 1968;24:905–8.